



Two shell collisions in the GRB afterglow phase

A. Vlasis¹, H.J. van Eerten², Z. Meliani¹, and R. Keppens^{1,3,4}

¹ Center for Plasma Astrophysics, K.U.Leuven, Belgium

² Center for Cosmology and Particle Physics, Physics Department, New York University, New York, NY 10003

³ FOM Institute for Plasma Physics Rijnhuizen, Nieuwegein, The Netherlands

⁴ Astronomical Institute, Utrecht University, The Netherlands

Abstract. Strong optical and X-Ray flares often appear in the afterglow phase of Gamma-Ray Bursts (GRBs). We perform high resolution numerical simulations of late collisions between two ultra-relativistic shells in order to explore these events. Such consecutive shells can be formed due to the variability in the central source of a GRB. We examine the case where a cold uniform shell collides with a self similar relativistic, shocked shell (Blandford & McKee 1976) in a constant density environment. We produce the corresponding light curves for the afterglow phase and examine the occurrence and chromaticity of optical and radio flares assuming different opening angles. We conclude that occurrence of optical and radio flares is possible for small opening angles of the jet. For our simulations we use the Adaptive Mesh Refinement version of the Versatile Advection Code (Keppens et al. 2003; Meliani et al. 2008) while the synchrotron radiation has been calculated with the method introduced in Van Eerten & Wijers (2009).

Key words. Gamma rays: hydrodynamics – Gamma rays: collisions – Radiation : Synchrotron – Radiation : light curves – Radiation: emission images

1. Introduction

Gamma-Ray Bursts (GRBs) are signaling catastrophic events like mergers, neutron star - neutron star or black hole - neutron star (short GRBs), or collapsing massive stars (long GRBs). Colliding ultra-relativistic shells emerge, and according to the internal collision model (Rees & Mészáros 1994), fluctuations in the Lorentz factor of the ejected medium give rise to internal shock collisions whenever a fast part of the ejecta catches up with a slower one. Gamma rays are the result of the conversion of the kinetic energy of ultra-relativistic particles to radiation at the shock region. The duration of long GRBs is ~ 10 s,

but the energy content of the explosion is less well constrained and depends on the geometry of the explosion. A spherical explosion in that timescale would imply an unreasonably high amount of energy of the order of 10^{54} ergs for the ejected material. Therefore a jet structured outflow which requires much less energy ($\sim 10^{52}$ ergs) is often assumed.

It is now widely accepted that the GRB afterglows are produced when the initially ejected outflow decelerates in the interstellar medium and the shock accelerated electrons lose their energy by means of synchrotron radiation (Sari et al. 1998). The standard fireball model, consisting of one relativistic blast

wave propagating in the interstellar medium (ISM), predicts smooth afterglow light curves. However, recent observations in X-ray, optical and radio reveal occasional rebrightenings of light curves at both early and late times that cannot be explained without altering the standard model.

It has been proposed that variations in the external density could result in the appearance of variability in the afterglow light curves (Lazzati et al. 2002). Simulations of an expanding blast wave through a medium with density bumps have been performed for spherical explosions (Nakar & Granot 2007; Van Eerten et al. 2009), resulting in a smooth flux decay in the light curve rather than a sharp flare.

A second mechanism that could explain the observed variability is energy injection in the afterglow shock (Rees & Mészáros 1994). In that model a second blast wave, emitted from the central source at a later time and after the prompt γ -rays emission has occurred, catches up with the afterglow shock which leads to a rebrightening of the light curve. Although the internal shock collision models require time scales within the timeframe of the prompt emission, late collision models imply a prolonged activity of the central engine. As proposed recently, fragmentation of the progenitor in the form of a self-gravitating neutron lump and subsequent accretion during the collapse of a rapidly rotating stellar core (King et al. 2005) can be a mechanism to obtain late activity from the central engine.

2. Modeling the two shell collisions

We use the AMRVAC code (Keppens et al. 2003; Meliani et al. 2008) to solve the special relativistic hydrodynamics equations in 1D spherical symmetry. We perform high resolution numerical simulations of a pulse catching up at late time with the forward shock, which is modeled using the Blandford & McKee self-similar solution for an ultra-relativistic strong explosion (Blandford & McKee 1976). We use a domain of size $[0.01, 10] \times 10^{18}$ cm and 240 cells in the coarsest level of refinement and reach a maximum of 22 levels, where each

level doubles the resolution leading to an effective resolution of 5×10^8 cells.

We consider a BM shell propagating into a cold ISM (number density $n_1 = 1 \text{ cm}^{-3}$, pressure $p_1 = 10^{-5} n_1 m_p c^2$), and a second shell following at a distance $\Delta R = 10^{14}$ cm behind the BM shell, as shown in the top left panel of Fig. 1. Initially the BM shock has a Lorentz factor $\Gamma_{BM} = 23$ which is the same for the uniform shell, $\Gamma_U = 23$, and the energy of the two shells is chosen identical, $E_{BM} = E_U = 10^{52}$ erg.

In Fig. 1 we show the evolution of the two shell system. At early stages a reverse shock crosses the second shell, transforming part of its kinetic energy into thermal energy. That leads to a fast deceleration of the second shell. Meanwhile, its forward shock propagates into the BM medium by continuously heating the matter it encounters. The BM shock decelerates fast in its usual self-similar manner as it traverses the ISM medium. At emission time $t_e = 2.345 \times 10^7$ sec the forward shock has reached the BM one and the two shell system now behaves as one merged shell. The remainder of the second shell, having lost most of its kinetic energy, now propagates with a very small Lorentz factor ~ 1 and the separation distance from the merged shell continuously increases.

3. Radiation calculations

In this section we use the radiation code introduced in Van Eerten & Wijers (2009) to calculate the received flux for a given observer frequency. The electrons accelerated at the shock region emit their energy by means of synchrotron radiation. In the present calculations we construct optical and radio light curves by taking into account a synchrotron self-absorption mechanism (s.s.a.) for the photons that are re-absorbed from the synchrotron electrons, but we do not take into account emission from Compton scattering or the effects from electron cooling.

In both external and internal collision models, synchrotron radiation requires the existence of magnetic field at the shock region. At the shock front electrons are accelerated to relativistic velocities and small scale magnetic

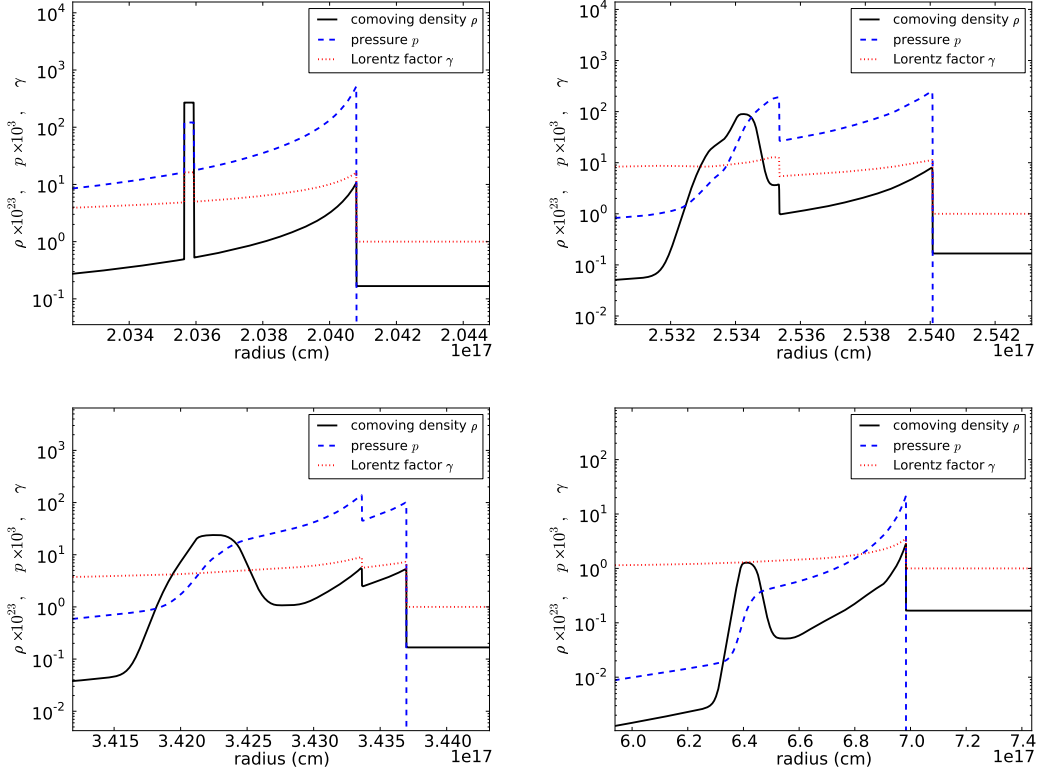


Fig. 1. Snapshots of the dynamics, taken at emission times $t_e = 6.809009 \times 10^6$, $t_e = 8.477 \times 10^6$, $t_e = 1.480 \times 10^7$ and $t_e = 2.345 \times 10^7$ sec. (top left - bottom right). Density, pressure and Lorentz factor are indicated as the solid, dashed, and dotted line. The different phases of the collision are visible including the appearance of the forward shock at the early stages of the simulation, the separation from the second shell and the collision of the forward shock with the BM shell.

fields are created and we assume that their energy densities can be expressed as fractions of the thermal energy density according to

$$\epsilon_B \equiv \frac{U_B}{e_{th}}, \quad \epsilon_E \equiv \frac{U_E}{e_{th}},$$

where $U_B = B^2/8\pi$ and U_E are the magnetic and electron energy densities. Together with the fraction ξ_N of the available electrons that is accelerated, and the slope p of the resulting power law distribution, these quantities are used to parametrize the radiation code. In our case we set these parameters as $\epsilon_B = 0.01$, $\epsilon_E = 0.1$, $\xi_N = 0.1$ and $p = 2.5$. We calculate optical (5×10^{14} Hz) and radio (10^8 Hz) light curves, assuming both isotropic expan-

sion and collimated outflow. We approximate collimated outflow by taking a conic section from the spherical outflow result and assuming negligible lateral expansion of the jet occurs at the stages under consideration. In order to include the initial stages of the afterglow that are not covered by our simulation, we introduce in the code an analytical solution covering in observer time from 0.001 days, until the beginning of the simulation at 0.01 days.

The flaring activity as presented in the optical light curves follows three stages. A sudden rise at $t_{obs} = 0.23$ days, coinciding with the formation of the forward shock at the second shell, a weak decay that corresponds to the propagation of the forward shock of the second

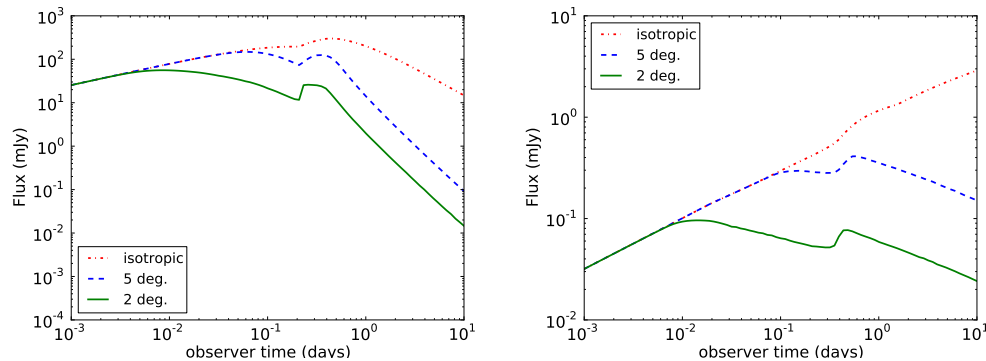


Fig. 2. Optical (left) and radio (right) light curves for the two shell system assuming isotropic and collimated outflow. The flaring activity is clearly visible for small opening angles.

shell into the BM shell, and a steep decay at $t_{obs} = 0.35$ days, which is the time the forward shock overtakes the BM shell. We also notice that the flaring activity is more pronounced in the case of small opening angles compared to the case of isotropic expansion. Simultaneous emission from different angles arrives at different observer times and will cause any feature in the light curve to become smoothed out. This effect is less severe the smaller the opening angle of the jet, and therefore the flares are more pronounced for jets with a small opening angle. In addition we notice a time difference in the occurrence of the optical and radio flare. This can be understood as follows. In the optical the jet is optically thin and the merger of the two shells can be seen as soon as the forward shock of the second shell is created while propagating in the BM shell. In the radio the jet is optically thick due to s.s.a. and we only see the effect of the merger once it has nearly completed. This results in a plateau in the optical flare and a sharp peak in the radio flare.

4. Conclusions

We have performed high resolution numerical simulations of two ultra-relativistic shells colliding in the afterglow phase and constructed optical and radio light curves for different jet opening angles. We show that there is a straightforward connection between the dynamics of the flow and the flux variability in

the light curves and claim that the chromaticity of the flare is a direct result of the s.s.a. mechanism and the angle dependence of the emission. We conclude that a flare is possible to occur in both optical and radio frequencies as long as the opening angle of the jet remains small. An extended work taking into account different energy and Lorentz factor for the second shell is expected to reveal more on the dependence of the flare on the characteristics of the flow.

References

- Blandford, R. D., & McKee, C. F. 1976, *Phys. Fluids*, 19, 1130.
- Keppens, R. et al. 2003, *Comp. Phys. Commun.*, 153, 317
- Meliani, Z. et al. 2007, *MNRAS*, 376, 1189-1200
- King, A. et al. 2005, *ApJ*, 630, L113
- Lazzati et al. 2002, *A&A* 396, L5
- Nakar, E. & Granot, J. 2007, *MNRAS*, 380, 1744
- Rees, M. J., & Mészáros, P. 1994, *ApJ*, 430, L93
- Rees, M. J., & Mészáros, P. 1998, *ApJ*, 496, L1
- Sari, R., et al. 1998 *ApJ*, 497, L17-L20
- Van Eerten, H. J., & Wijers, R. A. M. J. 2009, *MNRAS*, 394, 2164
- Van Eerten, H. J., et al. 2009, *MNRAS*, 398, L63